

ENERGY BALANCE RELATIONS FOR FLOW THROUGH THICK POROUS STRUCTURES

SANTANU KOLEY & KOTTALA PANDURANGA

Department of Mathematics, Birla Institute of Technology and Science – Pilani, Hyderabad Campus, India.

ABSTRACT

In wave–structure interaction problems, energy balance relations are often derived and used to check the accuracy of the computational results obtained using numerical methods. These energy identities are also used to get qualitative information about various physical quantities of interest. It is well known that for rigid structures, the energy identity is $K_r^2 + K_t^2 = 1$, where K_r and K_t are the reflection and transmission coefficients, respectively. Even if we take flexible barriers, then also the aforementioned energy identity will hold. Now, for wave past a thick porous structure, often a major portion of the incoming wave energy is dissipated due to the structural porosity. So, the aforementioned energy identity will be modified into $K_r^2 + K_t^2 + K_D = 1$, where K_D takes into account the amount of dissipative wave energy. These energy identities are available in the literature for thin porous barriers. But derivation of the energy identity is complicated for thick porous structures due to complex momentum equation and boundary conditions. In the present paper, an appropriate energy identity will be derived for water waves past a thick rectangular porous structure. In this regard, Green's second identity is used in multi-domain regions with the arguments velocity potential and its complex conjugate. With the help of complex function theory, the final form of the same is written in a compact form. Now, to compute each quantity associated with the energy identity, the associated boundary value problem is converted into a system of Fredholm integral equations. Finally, using the boundary element method, the components present in the energy identity are obtained and checked for validation.

Keywords: boundary element method, energy identity, Green's function, integral equation, water waves.

1 INTRODUCTION

In recent decades, thick porous structures such as rubble mound breakwaters are used in harbors for the protection of various marine infrastructures. Due to the presence of structural porosity, these types of breakwaters can dissipate a major part of the incoming wave energy. This process helps to create a tranquillity zone in the lee side of these breakwaters. The impact of the waves on these types of structures is less compared to the conventional upright, rigid, impermeable breakwaters. Sollitt and Cross [1] presented a mathematical model to analyze the gravity wave interaction with thick porous structures over uniform bottom bed. In this work, an analytical solution based on eigenfunction expansions method is used to solve the associated boundary value problem (BVP). A similar analytical solution technique was used by the authors of [2–8], etc. In most of the aforementioned papers, complex dispersion relations in the structural domain are used. The major difficulty lies in finding the complex roots of the complex dispersion relations accurately. However, few methods and related algorithms have been proposed to find out the nature and the locations of the roots of the aforementioned complex dispersion relation [3, 9, 10]. On the other hand, for wave interaction with thick porous structures of arbitrary shape and seabed undulation, a numerical solution technique based on the boundary element method (BEM) has been developed and used by many researchers (see [11–16], etc.). In some of the aforementioned studies, the BEM is suitably coupled with the eigenfunction expansion method (EEM) for faster convergence and computational efficiency. One of the biggest advantages of using BEM is that it does not need the dispersion relation in the structural domain.

To assess the effectiveness of these thick porous structures as a breakwater, often quantification of the amount of dissipated wave energy by these structures is needed. Further, to validate the computational results and to show the accuracy of the numerical computations, often energy balance relations are established. It is well known that, in case of thin/thick impervious structures, the reflection and transmission coefficients and , respectively, will satisfy the energy identity $K_r^2 + K_t^2 = 1$ [17, 18]. However, in the presence of structural porosity, a major portion of the incoming wave energy is dissipated and the energy identity is modified to $K_r^2 + K_t^2 + K_D = 1$, in which the term is related to the wave energy dissipation due to the structural porosity (see [19–21]). Although the aforementioned relation is used to quantify the energy dissipation, a theoretical derivation for the same is not available in the literature.

In the present paper, our main aim is to derive an energy identity theoretically for oblique water waves scattered by a thick porous structure in finite water depth. The thick porous structure considered here is having a geometry similar to a trapezoidal shape porous breakwater. Green’s second identity is used to derive an expression for the energy balance relation. To compute each term associated with the energy identity, the associated BVP is solved using BEM. Finally, the validation of the derived energy balance relation and the accuracy of the numerical solutions are presented.

2 MATHEMATICAL FORMULATION

The physical problem is analyzed in Cartesian co-ordinate system in water of finite depth under the assumption of linearized water wave theory. It is assumed that the incident wave is coming from x -direction and makes an angle θ with the x -axis (Fig. 1). Further, the motion of water is assumed to be simple harmonic in time with the angular frequency ω . This assumption ensures that the velocity potential $\Phi(x, y, z, t)$ exists and will take the form $\Phi(x, y, z, t) = \Re e \left\{ \phi(x, z) e^{i(k_y y - \omega t)} \right\}$, where $\phi(x, z)$ is the spatial coordinate-dependent velocity potential and $k_y = k_0 \sin \theta$ with k_0 being the progressive wave mode in the open water region. Due to the presence of thick porous structure, the total water domain is divided into the three regions, R_1 , R_2 , and R_3 , as shown in Fig. 1. Thus, $\phi_j(x, z)$ for $j=1,2,3$ satisfies the reduced wave equation

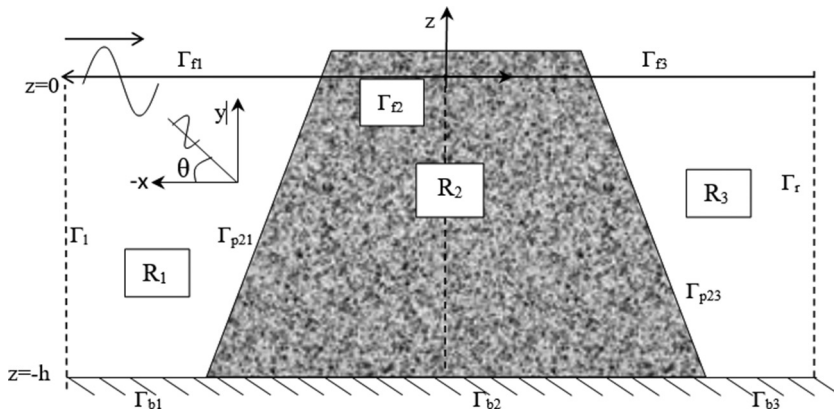


Figure 1: Cross section of the porous breakwater.

$$\left(\frac{\partial^2}{\partial x^2} + \frac{\partial^2}{\partial z^2} - k_y^2 \right) \phi_j = 0. \tag{1}$$

The boundary conditions at the free surface are given by

$$\begin{cases} \frac{\partial \phi_j}{\partial n} - K \phi_j = 0, & \text{on } \Gamma_{fj} \text{ for } j=1,3, \\ \frac{\partial \phi_2}{\partial n} - K(m_2 + if_2)\phi_2 = 0, & \text{on } \Gamma_{f2}, \end{cases} \tag{2}$$

where $K = \omega^2 / g$ and $\partial / \partial n$ represents the normal derivative. Further, the bottom boundary conditions will take the form

$$\frac{\partial \phi_j}{\partial n} = 0 \text{ on } \Gamma_{bj} \text{ for } j = 1, 2, 3. \tag{3}$$

The continuity of water pressure and normal velocity at fluid structure interfaces Γ_{p21} and Γ_{p23} are given by

$$\begin{cases} \phi_j = (m_2 + if_2)\phi_2, \\ \frac{\partial \phi_j}{\partial n} = -\varepsilon_2 \frac{\partial \phi_2}{\partial n}, \end{cases} \text{ on } \Gamma_{p2j} \text{ for } j = 1, 3, \tag{4}$$

where ε_2 , m_2 and f_2 are porosity, inertial and friction coefficients of the porous region R_2 (see [1] for further details). The value m_2 can be calculated using the formula $m_2 = \{1 + (1 - \varepsilon_2)C_{M2} / \varepsilon_2\}$, where C_{M2} is the added mass coefficient for the region. The expression for the friction coefficient is given by

$$f_2 = \frac{1}{\omega} \frac{\int_{R_2} d\Omega \int_t^{t+T} \left\{ \frac{\varepsilon_2^2 v_2 |\bar{q}_2|^2}{K_{P2}} + \frac{\varepsilon_2^3 C_{f2}}{\sqrt{K_{P2}}} |\bar{q}_2|^3 \right\} dt}{\int_{R_2} d\Omega \int_t^{t+T} \varepsilon_2 |\bar{q}_2|^2 dt}, \tag{5}$$

where \bar{q}_2, v_2, K_{P2} and C_{f2} are the seepage velocity, kinematic viscosity, intrinsic permeability, and dimensionless turbulence resistance coefficient, respectively, for the porous region R_2 . Finally, the far-field boundary conditions are given by

$$\begin{cases} \phi_1(x, z) = e^{ik_x x} \psi_0(k_0, z) + R e^{-ik_x x} \psi_0(k_0, z) & \text{as } x \rightarrow -\infty, \\ \phi_3(x, z) = T e^{ik_x x} \psi_0(k_0, z) & \text{as } x \rightarrow \infty, \end{cases} \tag{6}$$

where R and T are the coefficients associated with reflection and transmitted waves, respectively. Now, to apply the BEM, the domain must be closed. Therefore, without loss of generality, two auxiliary boundaries (as seen in Fig. 1) are chosen at a distance far away from the structure. Thus, eqn (6) can be rewritten as

$$\begin{cases} \frac{\partial(\phi_1 - \phi_0)}{\partial n} - ik_x(\phi_1 - \phi_0) = 0, & \text{on } \Gamma_l \\ \frac{\partial \phi_3}{\partial n} - ik_x \phi_3 = 0, & \text{on } \Gamma_r \end{cases}, \tag{7}$$

with ϕ_0 representing the incident wave potential and it takes the form $\phi_0 = e^{ik_x x} \psi_0(k_0, z)$, with

$$\psi_0(k_0, z) = \frac{\cosh k_0(z+h)}{N_0}, \quad N_0^2 = \frac{2k_0 h + \sinh(2k_0 h)}{4k_0}.$$

Here, k_0 is the real positive root of the dispersion relation $K = k \tanh(kh)$ and $k_x = k_0 \cos \theta$. This dispersion relation has infinite number of roots and out of these, we are taking only the positive real root, and an infinite number of purely imaginary roots lie on the upper half complex plane. The vertical eigenfunctions $\psi_n(k_n, z)$ will satisfy the following orthonormal relation:

$$\int_{-h}^0 \psi_m(k_m, z) \psi_n^*(k_n, z) dz = \delta_{mn}, \tag{8}$$

where $\psi_n^*(k_n, z)$ represents the complex conjugate of $\psi_n(k_n, z)$.

3 ENERGY BALANCE RELATIONS

In this section, the energy identities or energy balance relations for the BVP as described in Section 2 are derived using the Green’s second identity. Applying Green’s second identity to $\phi(x, z)$ and $\phi^*(x, z)$ in each of the three regions as shown in Fig. 1, we get the following identity:

$$\int_{\Gamma} \left(\phi \frac{\partial \phi^*}{\partial n} - \phi^* \frac{\partial \phi}{\partial n} \right) d\Gamma = 0, \tag{9}$$

where Γ represents the boundaries of the regions R_j for $j = 1, 2, 3$ as shown in Fig. 1. Consider the closed contours Γ_i for $i = 1, 2, 3$ as shown in Fig. 1, where each Γ_i is taken as the following:

$$\begin{aligned} \Gamma_1 &= \Gamma_1 \cup \Gamma_{b1} \cup \Gamma_{p21} \cup \Gamma_{f1} \\ \Gamma_2 &= \Gamma_{p21} \cup \Gamma_{b2} \cup \Gamma_{p23} \cup \Gamma_{f2} \\ \Gamma_3 &= \Gamma_{p23} \cup \Gamma_{b3} \cup \Gamma_r \cup \Gamma_{f3} \end{aligned} \tag{10}$$

Now, the integral in eqn (9) is evaluated over each boundary using the boundary conditions in eqns (2)–(7). It is to be noted that $\phi(x, z)$ and $\phi^*(x, z)$ will satisfy the same boundary conditions on each boundary with appropriate modifications. Thus, the contributions from each boundary are as follows:

$$\int_{\Gamma_{bi}} \left(\phi_i \frac{\partial \phi_i^*}{\partial n} - \phi_i^* \frac{\partial \phi_i}{\partial n} \right) d\Gamma_i = 0 \quad \text{for } i = 1, 2, 3, \tag{11}$$

$$\int_{\Gamma_{fi}} \left(\phi_i \frac{\partial \phi_i^*}{\partial n} - \phi_i^* \frac{\partial \phi_i}{\partial n} \right) d\Gamma_i = 0 \quad \text{for } i = 1, 3. \tag{12}$$

Consequently, we can obtain the following relations after applying the orthogonality relationship between ψ_0 and ψ_0^*

$$\int_{\Gamma_1} \left(\phi_1 \frac{\partial \phi_1^*}{\partial n} - \phi_1^* \frac{\partial \phi_1}{\partial n} \right) d\Gamma_1 = 2i k_x (1 - |R|^2), \tag{13}$$

$$\int_{\Gamma_r} \left(\phi_3 \frac{\partial \phi_3^*}{\partial n} - \phi_3^* \frac{\partial \phi_3}{\partial n} \right) d\Gamma_3 = -2i k_x (|T|^2), \quad (14)$$

$$\int_{\Gamma_{f2}} \left(\phi_2 \frac{\partial \phi_2^*}{\partial n} - \phi_2^* \frac{\partial \phi_2}{\partial n} \right) d\Gamma_2 = Kf_2 \int_{\Gamma_{f2}} |\phi_2|^2 d\Gamma_2. \quad (15)$$

Adding all the contributions as in eqns (11)–(15) and using the interface conditions as in eqn (4), we get the following energy balance relations:

$$\Im m \int_{\Gamma_{p21}} \left(\phi_1 \frac{\partial \phi_1^*}{\partial n} \right) d\Gamma_1 = k_x (|R|^2 - 1), \quad (16)$$

$$\Im m \int_{\Gamma_{p23}} \left(\phi_3 \frac{\partial \phi_3^*}{\partial n} \right) d\Gamma_3 = -k_x (|T|^2), \quad (17)$$

$$\Im m \left\{ \left(\frac{1}{a\varepsilon_2} \right) \left[\int_{\Gamma_{p21}} \left(\phi_1 \frac{\partial \phi_1^*}{\partial n} \right) d\Gamma_1 - \int_{\Gamma_{p23}} \left(\phi_3 \frac{\partial \phi_3^*}{\partial n} \right) d\Gamma_3 \right] \right\} = Kf_2 \int_{\Gamma_{f2}} |\phi_2|^2 d\Gamma_2, \quad (18)$$

with $a = (m_2 + if_2)$. Simplifying eqn (18) and using eqns (16) and (17), we get the form of the energy balance relation as

$$\Xi = |R|^2 + |T|^2 + K_D = 1, \quad (19)$$

where K_D is given by

$$K_D = - \left[\frac{Kf_2 \varepsilon_2}{m_2 k_x} |a|^2 \int_{\Gamma_{f2}} |\phi_2|^2 d\Gamma_2 + \frac{f_2}{m_2 k_x} \Re e \left\{ \int_{\Gamma_{p21}} \left(\phi_1 \frac{\partial \phi_1^*}{\partial n} \right) d\Gamma_1 - \int_{\Gamma_{p23}} \left(\phi_3 \frac{\partial \phi_3^*}{\partial n} \right) d\Gamma_3 \right\} \right].$$

4 BOUNDARY ELEMENT METHOD

The unknown velocity potential and its normal derivative in the interior and boundary of a domain can be obtained by applying the Green's second identity to $\phi(x, z)$ and the Green's function $G(x, z; \xi, \eta)$ and the form of the same will be

$$\begin{pmatrix} \phi(\xi, \eta) \\ \frac{1}{2} \phi(\xi, \eta) \end{pmatrix} = \int_{\Gamma} \left(\phi \frac{\partial G}{\partial n} - G \frac{\partial \phi}{\partial n} \right) d\Gamma, \quad \begin{pmatrix} \text{if } (\xi, \eta) \in \Omega \setminus \Gamma \\ \text{if } (\xi, \eta) \in \Gamma \end{pmatrix}. \quad (20)$$

In eqn (20), $G(x, z; \xi, \eta)$ satisfies

$$\left(\frac{\partial^2}{\partial x^2} + \frac{\partial^2}{\partial z^2} - k_y^2 \right) G = -\delta(x - \xi) \delta(z - \eta). \quad (21)$$

The expression for $G(x, z, \xi, \eta)$ is given by

$$G = \frac{-K_0(k_y r)}{2\pi}, \quad r = \sqrt{(x - \xi)^2 + (z - \eta)^2}, \tag{22}$$

where K_0 is the modified Bessel function of the second kind and is of zeroth order. Now, $\partial G / \partial n$ can be obtained by using the following formula

$$\frac{\partial G}{\partial n} = \frac{k_y}{2\pi} K_1(k_y r) \frac{\partial r}{\partial n}, \tag{23}$$

where K_1 is the modified Bessel function of the second kind and is of first order. Employing the boundary conditions, i.e. eqns (2)–(7) into eqn (20) for each of the regions R_j for $j = 1, 2, 3$, we get the following integral equations:

$$-\frac{1}{2} \phi_1(\xi, \eta) + \int_{\Gamma_1} \left(\frac{\partial G}{\partial n} - ik_x G \right) \phi_1 d\Gamma + \int_{\Gamma_{b1}} \frac{\partial G}{\partial n} \phi_1 d\Gamma + \int_{\Gamma_{p21}} \left(\phi_1 \frac{\partial G}{\partial n} - G \frac{\partial \phi_1}{\partial n} \right) d\Gamma + \int_{\Gamma_{f1}} \left(\frac{\partial G}{\partial n} - KG \right) \phi_1 d\Gamma = \int_{\Gamma_1} \left(\frac{\partial \phi_0}{\partial n} - ik_x \phi_0 \right) G, \tag{24}$$

$$-\frac{1}{2} \phi_2(\xi, \eta) + \int_{\Gamma_{p21}} \left(\frac{1}{a} \frac{\partial G}{\partial n} \phi_1 + \frac{G}{\varepsilon_2} \frac{\partial \phi_1}{\partial n} \right) d\Gamma + \int_{\Gamma_{p23}} \left(\frac{1}{a} \frac{\partial G}{\partial n} \phi_3 + \frac{G}{\varepsilon_2} \frac{\partial \phi_3}{\partial n} \right) d\Gamma + \int_{\Gamma_{b2}} \frac{\partial G}{\partial n} \phi_1 d\Gamma + \int_{\Gamma_{f2}} \left(\frac{\partial G}{\partial n} - KaG \right) \phi_2 d\Gamma = 0 \tag{25}$$

$$-\frac{1}{2} \phi_3(\xi, \eta) + \int_{\Gamma_{p23}} \left(\phi_3 \frac{\partial G}{\partial n} - G \frac{\partial \phi_3}{\partial n} \right) d\Gamma + \int_{\Gamma_{b3}} \frac{\partial G}{\partial n} \phi_3 d\Gamma + \int_{\Gamma_r} \left(\frac{\partial G}{\partial n} - ik_x G \right) \phi_3 d\Gamma + \int_{\Gamma_{f3}} \left(\frac{\partial G}{\partial n} - KG \right) \phi_3 d\Gamma = 0. \tag{26}$$

The above system of integral equations is converted into the system of linear algebraic equations using BEM. Here, the boundaries of the regions R_j for $j = 1, 2, 3$, are discretized into finite number of boundary elements with the assumption that the values of ϕ and $\partial \phi / \partial n$ are constants over each element. Under the above assumptions, we can get the following system of algebraic equations:

$$\Sigma \left(H^{ij} - ik_x G^{ij} \right) \phi_{1j} \Big|_{\Gamma_1} + \Sigma H^{ij} \phi_{1j} \Big|_{\Gamma_{b1}} + \Sigma \left(H^{ij} \phi_{1j} - G^{ij} \frac{\partial \phi_{1j}}{\partial n} \right) \Big|_{\Gamma_{p21}} + \tag{27}$$

$$\Sigma \left(H^{ij} - KG^{ij} \right) \phi_{1j} \Big|_{\Gamma_{f1}} = \Sigma \left(\frac{\partial \phi_{0j}}{\partial n} - ik_x \phi_{0j} \right) G^{ij} \Big|_{\Gamma_1}$$

$$\Sigma \left(\frac{1}{a} H^{ij} \phi_{1j} + \frac{1}{\varepsilon_2} G^{ij} \frac{\partial \phi_{1j}}{\partial n} \right) \Big|_{\Gamma_{p21}} + \Sigma \left(\frac{1}{a} H^{ij} \phi_{3j} + \frac{1}{\varepsilon_2} G^{ij} \frac{\partial \phi_{3j}}{\partial n} \right) \Big|_{\Gamma_{p23}} + \tag{28}$$

$$\Sigma H^{ij} \phi_{2j} \Big|_{\Gamma_{b2}} + \Sigma \left(H^{ij} - KaG^{ij} \right) \phi_{2j} \Big|_{\Gamma_{f2}} = 0$$

$$\begin{aligned} & \Sigma \left(H^{ij} \phi_{3j} - G^{ij} \frac{\partial \phi_{3j}}{\partial n} \right) \Big|_{\Gamma_{p23}} + \Sigma H^{ij} \phi_{3j} \Big|_{\Gamma_{b3}} + \Sigma (H^{ij} - ik_x G^{ij}) \phi_{3j} \Big|_{\Gamma_r} + \\ & \Sigma (H^{ij} - KG^{ij}) \phi_{3j} \Big|_{\Gamma_{f3}} = 0, \end{aligned} \tag{29}$$

where

$$H^{ij} = -\frac{1}{2} \delta_{ij} + \int_{\Gamma_j} \frac{\partial G}{\partial n} d\Gamma, \quad G^{ij} = \int_{\Gamma_j} G d\Gamma, \quad \delta_{ij} = \begin{cases} 1 & (i = j) \\ 0 & (i \neq j) \end{cases}$$

and are termed as influence coefficients. These coefficients are evaluated numerically using Gauss–Legendre quadrature formulae. Now, to get the matrix form, the point collocation method is used. In this method, the source point (ζ, η) will run over all the boundary elements and this will finally result in a system of M equations with M number of unknowns (M is the total number of boundary elements). Finally, the system eqns (27)–(29) are written in matrix form as

$$\begin{aligned} & ([H] - ik_x [G])[\phi] \Big|_{\Gamma_1} + ([H])[\phi] \Big|_{\Gamma_{b1}} + [H][\phi] - [G] \left[\frac{\partial \phi}{\partial n} \right] \Big|_{\Gamma_{p21}} + \\ & ([H] - K[G])[\phi] \Big|_{\Gamma_{f1}} = \left(\left[\frac{\partial \phi_0}{\partial n} \right] - ik_x [\phi_0] \right) [G] \Big|_{\Gamma_1} \end{aligned} \tag{30}$$

$$\begin{aligned} & \left(\frac{1}{\alpha} [H][\phi] + \frac{1}{\varepsilon_2} [G] \left[\frac{\partial \phi}{\partial n} \right] \right) \Big|_{\Gamma_{p21}} + \left(\frac{1}{\alpha} [H][\phi_3] + \frac{1}{\varepsilon_2} [G] \left[\frac{\partial \phi_3}{\partial n} \right] \right) \Big|_{\Gamma_{p23}} + \\ & ([H])[\phi_2] \Big|_{\Gamma_{b2}} + ([H] - K\alpha[G])[\phi_2] \Big|_{\Gamma_{f2}} = 0, \end{aligned} \tag{31}$$

$$\begin{aligned} & [H][\phi_3] - [G] \left[\frac{\partial \phi_3}{\partial n} \right] \Big|_{\Gamma_{p23}} + ([H])[\phi_3] \Big|_{\Gamma_{b3}} + ([H] - ik_x [G])[\phi_3] \Big|_{\Gamma_r} + \\ & ([H] - K[G])[\phi_3] \Big|_{\Gamma_{f3}} = 0, \end{aligned} \tag{32}$$

These eqns (30)–(32) are solved to obtain ϕ and $\partial\phi / \partial n$ over each boundary element. These values are used to determine the physical parameters of interest like reflection and transmission coefficients, free surface elevation, etc.

5 RESULTS AND DISCUSSION

In this section, various quantities present in the energy balance relation as in eqn (19) are evaluated using BEM as discussed in Section 4. The values of the parameters associated with wave and structure are taken as follows: $T = 10 \text{ sec}$ (T is the incident wave period), $h = 15$, $\tan\alpha = 1/1.5$ (α is the sloping angle of the trapezoidal breakwater), b/h (b is the

Table 1: Comparative study of various quantities associated with eqn (19) for various values of θ and k_0h .

k_0h	θ	$ R $	$ T $	K_D	Ξ
0.5	30	0.5389	0.4003	0.5494	1.0000
	45	0.4620	0.4027	0.6243	0.9999
	60	0.3466	0.4093	0.7124	1.0000
1.0	30	0.3944	0.1905	0.8082	1.0000
	45	0.4059	0.1694	0.8066	1.0000
	60	0.4464	0.1436	0.7801	0.9999
2.0	30	0.3766	0.0225	0.8577	1.0000
	45	0.3784	0.0187	0.8564	0.9999
	60	0.4310	0.0147	0.8140	0.9999
3.0	30	0.3929	0.0030	0.8456	0.9999
	45	0.4084	0.0021	0.8332	0.9999
	60	0.4158	0.0017	0.8271	0.9999
4.0	30	0.4211	0.0004	0.8227	1.0000
	45	0.4450	0.0003	0.8019	0.9999
	60	0.4730	0.0002	0.7763	1.0000

width of the breakwater at the free surface), $\theta = 45^\circ$ (in the angle of incidence of the incident wave), $m_2 = 1.0$, $f_2 = 1.0$, $\varepsilon_2 = 0.3$ unless otherwise mentioned.

In Table 1, the numerical values of the components present in the energy identity as given in eqn (19) are provided for different values of dimensionless wave number k_0h and angle of incidence θ . Further, in Table 2, the same quantities are provided for various values of k_0h and porosity ε_2 . It is observed from the two tables that the sum of $|R|^2 + |T|^2 + K_D = 1$ and this clearly shows the validity of the energy balance relation given in eqn (19).

6 CONCLUSIONS

In the present study, the energy balance relation for water waves past a thick porous structure is derived. The associated BVP is solved numerically using BEM. Finally, by calculating the values of each quantity associated with the derived energy balance relation, the energy identity is validated. The solution methodology can easily be extended to derive energy identities for more complex problems that arise in different branches of mathematical physics.

ACKNOWLEDGEMENTS

Santanu Koley acknowledges the financial support received through the DST project DST/INSPIRE/04/2017/002460 to pursue this research work. Further, support was received from BITS-Pilani, Hyderabad Campus through the RIG project BITS/GAU/RIG/2019/H0631 and Additional Competitive Research Grant BITS/GAU/ACRG/2019/H0631.

Table 2: Comparative study of various quantities associated with eqn (19) for various values of ε_2 and k_0h .

k_0h	ε_2	$ R $	$ T $	K_D	Ξ
0.5	0.1	0.7716	0.2076	0.3615	0.9997
	0.3	0.4620	0.4027	0.6243	0.9999
	0.5	0.2754	0.4703	0.7030	1.0000
1.0	0.1	0.7270	0.0920	0.4630	0.9999
	0.3	0.4057	0.1694	0.8066	0.9999
	0.5	0.2288	0.1927	0.9105	0.9999
2.0	0.1	0.6996	0.0106	0.5104	0.9999
	0.3	0.3784	0.0187	0.8564	0.9999
	0.5	0.2181	0.0205	0.9520	0.9999
3.0	0.1	0.7199	0.0012	0.4818	1.0000
	0.3	0.4084	0.0021	0.8332	0.9999
	0.5	0.2495	0.0024	0.9378	1.0000
4.0	0.1	0.7523	0.0001	0.4340	0.9999
	0.3	0.4450	0.0003	0.8019	0.9999
	0.5	0.2739	0.0003	0.9250	1.0000

REFERENCES

- [1] Sollitt, C.K. & Cross, R.H., Wave transmission through permeable breakwaters. *Proceedings of the 13th International Conference on Coastal Engineering*. ASCE, pp. 1827–1846, 1972. <https://doi.org/10.1061/9780872620490.106>
- [2] Rojanakamthorn, S., Isobe, M. & Watanabe, A., Modeling of wave transformation on submerged breakwater. *Proceedings of the 22nd International Conference on Coastal Engineering*. ASCE, pp. 1060–1073, 1990. <https://doi.org/10.1061/9780872627765.082>
- [3] Dalrymple, R.A., Losada, M.A. & Martin, P.A., Reflection and transmission from porous structures under oblique wave attack. *Journal of Fluid Mechanics*, **224**, pp. 625–644, 1991. <https://doi.org/10.1017/s0022112091001908>
- [4] Yu, X. & Chwang, A.T., Wave motion through porous structures. *Journal of Engineering Mechanics*, **120(5)**, pp. 989–1008, 1994. [https://doi.org/10.1061/\(asce\)0733-9399\(1994\)120:5\(989\)](https://doi.org/10.1061/(asce)0733-9399(1994)120:5(989))
- [5] Losada, I.J., Silva, R. & Losada, M.A., 3-D non-breaking regular wave interaction with submerged breakwaters. *Coastal Engineering*, **28(1–4)**, pp. 229–248, 1996. [https://doi.org/10.1016/0378-3839\(96\)00019-1](https://doi.org/10.1016/0378-3839(96)00019-1)
- [6] Liu, Y., Li, H.J. & Li, Y.C., A new analytical solution for wave scattering by a submerged horizontal porous plate with finite thickness. *Ocean Engineering*, **42**, pp. 83–92, 2012. <https://doi.org/10.1016/j.oceaneng.2012.01.001>
- [7] Liu, Y. & Li, H.J., Wave reflection and transmission by porous breakwaters: A new analytical solution. *Coastal Engineering*, **78**, pp. 46–52, 2013. <https://doi.org/10.1016/j.coastaleng.2013.04.003>

- [8] Behera, H. & Sahoo, T., Gravity wave interaction with porous structures in two-layer fluid. *Journal of Engineering Mathematics*, **87**(1), pp. 73–97, 2014. <https://doi.org/10.1007/s10665-013-9667-0>
- [9] Mendez, F.J. & Losada, I.J., A perturbation method to solve dispersion equations for water waves over dissipative media. *Coastal Engineering*, **51**(1), pp. 81–89, 2004. <https://doi.org/10.1016/j.coastaleng.2003.12.007>
- [10] Meylan, M.H. & Gross, L., A parallel algorithm to find the zeros of a complex analytic function. *ANZIAM Journal*, **44**, pp. 236–254, 2002. <https://doi.org/10.21914/anziamj.v44i0.495>
- [11] Sulisz, W., Wave reflection and transmission at permeable breakwaters of arbitrary cross-section. *Coastal Engineering*, **9**(4), pp. 371–386, 1985. [https://doi.org/10.1016/0378-3839\(85\)90018-3](https://doi.org/10.1016/0378-3839(85)90018-3)
- [12] Gu, Z.G. & Wang, H., Numerical modelling of wave energy dissipation within porous submerged breakwaters of irregular cross section. *Proceedings of the 23rd International Conference on Coastal Engineering, ASCE*, pp. 1189–1202, 1992.
- [13] Lee, J.F., A boundary element model for wave interaction with porous structures. *WIT Transactions on Modelling and Simulation*, Vol. 9, WIT Press: Southampton and Boston, pp. 145–152, 1995.
- [14] Koley, S., Behera, H. & Sahoo, T., Oblique wave trapping by porous structures near a wall. *Journal of Engineering Mechanics*, **141**(3), 04014122, pp. 1–15, 2015. [https://doi.org/10.1061/\(asce\)em.1943-7889.0000843](https://doi.org/10.1061/(asce)em.1943-7889.0000843)
- [15] Koley, S., Kaligatla, R.B. & Sahoo, T., Oblique wave scattering by a vertical flexible porous plate. *Studies in Applied Mathematics*, **135**(1), pp. 1–34, 2015. <https://doi.org/10.1111/sapm.12076>
- [16] Behera, H., Koley, S. & Sahoo, T., Wave transmission by partial porous structures in two-layer fluid. *Engineering Analysis with Boundary Elements*, **58**, pp. 58–78, 2015. <https://doi.org/10.1016/j.enganabound.2015.03.010>
- [17] Mei, C.C. & Black, J.L., Scattering of surface waves by rectangular obstacles in waters of finite depth. *Journal of Fluid Mechanics*, **38**(3), pp. 499–511, 1969. <https://doi.org/10.1017/s0022112069000309>
- [18] Porter, R. & Evans, D.V., Complementary approximations to wave scattering by vertical barriers. *Journal of Fluid Mechanics*, **294**, pp. 155–180, 1995. <https://doi.org/10.1017/s0022112095002849>
- [19] Gayen, R. & Mondal, A., A hypersingular integral equation approach to the porous plate problem. *Applied Ocean Research*, **46**, pp. 70–78, 2014. <https://doi.org/10.1016/j.apor.2014.01.006>
- [20] Chakraborty, R. & Mandal, B.N., Scattering of water waves by a submerged thin vertical elastic plate. *Archive of Applied Mechanics*, **84**(2), pp. 207–217, 2014. <https://doi.org/10.1007/s00419-013-0794-x>
- [21] Koley, S., Sarkar, A. & Sahoo, T., Interaction of gravity waves with bottom-standing submerged structures having perforated outer-layer placed on a sloping bed. *Applied Ocean Research*, **52**, pp. 245–260, 2015. <https://doi.org/10.1016/j.apor.2015.06.003>